

# Synergistic and Long-Lasting Wound Dressings Promote Multidrug-Resistant Staphylococcus Aureus-Infected Wound Healing

Xiangjie Fu<sup>1</sup>, Yaqiong Ni<sup>2</sup>, Guanchen Wang<sup>3</sup>, Runda Nie<sup>3</sup>, Yang Wang<sup>4</sup>, Run Yao<sup>1</sup>, Danyang Yan<sup>1</sup>, Mingming Guo<sup>3</sup>, Ning Li<sup>1</sup>

<sup>1</sup>Department of Blood Transfusion, National Clinical Research Center for Geriatric Disorders, Xiangya Hospital, Central South University, Changsha, 410008, People's Republic of China; <sup>2</sup>Hunan Provincial Key Laboratory of Micro&Nano Materials Interface Science, College of Chemistry and Chemical Engineering, Central South University, Changsha, 410083, People's Republic of China; <sup>3</sup>School of Chemistry and Chemical Engineering, Southwest University, Chongqing, 400715, People's Republic of China; <sup>4</sup>Institute of Integrative Medicine, Key Laboratory of Hunan Province for Liver Manifestation of Traditional Chinese Medicine, Xiangya Hospital, Central South University, Changsha, 410008, People's Republic of China

Correspondence: Ning Li, Tel +86 731 84327436, Email liningxy@csu.edu.cn

**Background:** Multidrug-resistant staphylococcus aureus infected wounds can lead to nonhealing, systemic infections, and even death. Although advanced dressings are effective in protecting, disinfecting, and maintaining moist microenvironments, they often have limitations such as single functionality, inadequate drug release, poor biosafety, or high rates of drug resistance.

**Methods:** Here, a novel wound dressing comprising glycyrrhizic acid (GA) and tryptophan-sorbitol carbon quantum dots (WS-CQDs) was developed, which exhibit synergistic and long-lasting antibacterial and anti-inflammatory effects. We investigated the characterization, mechanical properties, synergistic antibacterial effects, sustained-release properties, and cytotoxicity of GA/WS-CQDs hydrogels in vitro. Additionally, we performed transcriptome sequence analysis to elucidate the antibacterial mechanism. Furthermore, we evaluated the biosafety, anti-inflammatory effects, and wound healing ability of GA/WS-CQDs dressings using an in vivo mouse model of methicillin-resistant staphylococcus aureus (MRSA)-infected wounds.

**Results:** The prepared GA/WS-CQDs hydrogels demonstrated superior anti-MRSA effects compared to common antibiotics in vitro. Furthermore, the sustained release of WS-CQDs from GA/WS-CQDs hydrogels lasted for up to 60 h, with a cumulative release of exceeding 90%. The sustained-released WS-CQDs exhibited excellent anti-MRSA effects, with low drug resistance attributed to DNA damage and inhibition of bacterial biofilm formation. Notably, in vivo experiments showed that GA/WS-CQDs dressings reduced the expression of inflammatory factors (TNF- $\alpha$ , IL-1 $\beta$ , and IL-6) and significantly promoted the healing of MRSA-infected wounds with almost no systemic toxicity. Importantly, the dressings did not require replacement during the treatment process.

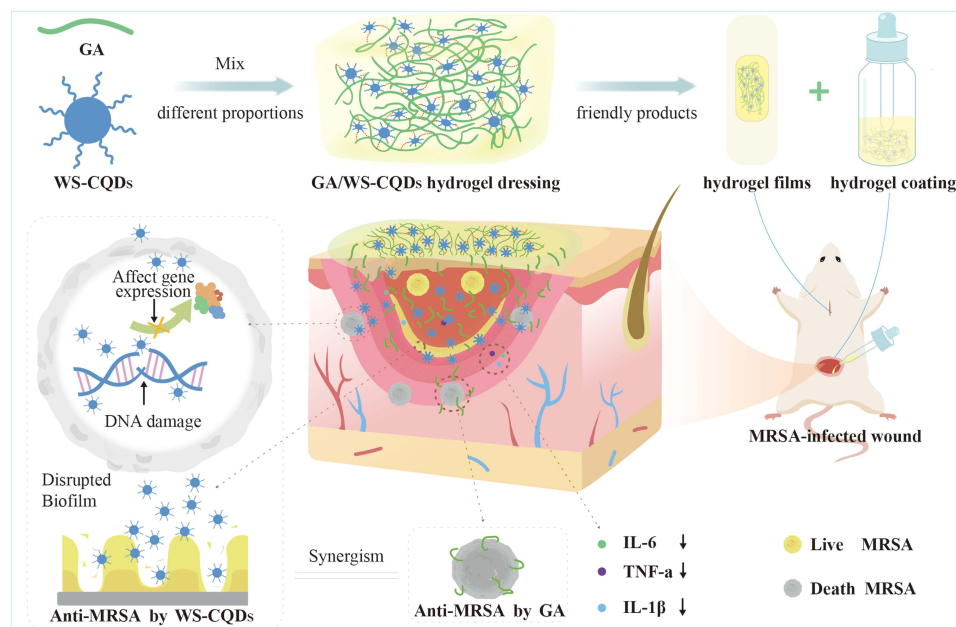
**Conclusion:** These findings emphasize the high suitability of GA/WS-CQDs dressings for MRSA-infected wound healing and their potential for clinical translation.

**Keywords:** tryptophan-sorbitol CQDs, glycyrrhizic acid, wound dressings, synergistic synergism, sustained release, methicillin-resistant staphylococcus aureus-infected wounds healing

## Introduction

Wounds infected with bacteria often result in nonhealing and serious complications, and in some cases, even death.<sup>1,2</sup> Globally, approximately 323,700 infections are caused by multidrug-resistant staphylococcus aureus, commonly known as “super-bacteria” each year. This led to 10,600 deaths and an estimated \$80 billion in total healthcare costs in global spending by 2024.<sup>3–5</sup> In clinical settings, methicillin-resistant staphylococcus aureus (MRSA) bacteria are found in over 40% of chronic wounds.<sup>6,7</sup> Unfortunately, MRSA is resistant to all known  $\beta$ -lactam antibiotics and many other common antibiotics, making the treatment of MRSA-infected wounds extremely challenging.<sup>7–9</sup> Therefore, there is a pressing need to develop antibiotic-free wound dressings with enhanced efficacy for the accelerated MRSA-infected wounds healing.

## Graphical Abstract



Hydrogels are three-dimensional (3D) networks consisting of physically or chemically cross-linked hydrophilic polymers, which are the best choice as a dressing material.<sup>10</sup> Their success as suitable wound dressings in the market is attributable to their highly porous, biocompatibility and tunable degradation, maintaining moist microenvironments, absorption of tissue exudates, and etc.<sup>11–13</sup> The structure and physicochemical properties of hydrogels can be adjusted by modifying the material composition, solution concentration, cross-linking method, and other factors.<sup>14,15</sup> Additionally, hydrogels can be functionalized by incorporating active antibacterial and anti-inflammatory substances.<sup>16,17</sup> Especially in recent years, related research has yielded many breakthroughs in enhancing the wound healing capacity of hydrogels.<sup>12,18</sup> The materials commonly used in the preparation of hydrogels include natural polymers such as chitosan, hyaluronic acid, alginate, or gelatin, and synthetic polymers such as polyethyleneglycol and polyvinylpyrrolidone.<sup>16</sup> At present, existing antibacterial hydrogels include those containing inorganic nanoparticles (eg, Ag NPs), hydrogels loaded with ciprofloxacin/gentamicin/vancomycin, and natural polymers with inherent antibacterial capabilities.<sup>17,19</sup> However, further efforts are still need to optimize the efficacy of hydrogels in MRSA-infected wound healing. For example, these limitations include the acceleration of wound adaptation and self-healing, drug selection and reasonably controlled release systems, enhancing antibacterial safety and ability, and improving the mechanical properties.<sup>18,20</sup>

With frontier developments of nanotechnology, the introduction of carbon quantum dots (CQDs) endows hydrogels with novel properties, such as improved mechanical strength, drug release, biological function, and etc.<sup>21</sup> CQDs, a class of zero-dimensional carbon-based nanomaterials, can attract much attention due to their water-solubility, ultrasmall size for direct renal excretion, and exceptional biocompatibility.<sup>22,23</sup> The properties and functions of CQDs can be manipulated in the stage of synthesis or post-modification. This enables outstanding advantages of CQDs for antibacterial applications and research. For instance, the low toxicity and low risk of drug resistance make CQDs highly promising antibacterial agents.<sup>24,25</sup> Importantly, CQDs contain many functional groups such as epoxy, carbonyl, hydroxyl, amine, and carboxyl on their surfaces and/or edges.<sup>26,27</sup> These features make them ideal building blocks for constructing CQDs-based hydrogel delivery system, where CQDs can interact with hydrogels through noncovalent interactions or chemically-linked networks.<sup>28–30</sup> Moreover, these properties combine the advantages of both hydrogels (eg, pore sizes, hydrophilicity, mechanics) and CQDs (eg, high surface area, chemical activity, aggregation-caused quenching, mechanics), presenting a win-win strategy.<sup>31–33</sup> While CQDs

have been incorporated into hydrogels as main components of antibacterial hydrogels,<sup>34,21</sup> but the combination therapy of CQDs and hydrogels has rarely been reported or applied in clinical settings.

Tryptophan-sorbitol carbon quantum dots (WS-CQDs) were synthesized through a one-pot hydrothermal method using natural tryptophan and sorbitol. Our team found that WS-CQDs exhibited good biocompatibility and great potential in biomedicine.<sup>35</sup> To our knowledge, it is crucial to possess both contact and release antibacterial capabilities to achieve lasting and durable effects for an ideal antibacterial wound dressing.<sup>36–38</sup> Additionally, their preparation, architecture, biocompatibility, biodegradability, encapsulation property, and intelligence need to be considerations.<sup>39–41</sup> In this study, we supposed that developing a wound dressing incorporating glycyrrhizic acid (GA) and WS-CQDs could serve as an effective strategy for improving the MRSA-infected wound healing process. GA, widely acquired from medicinal herbs, can self-assembly form a supramolecular hydrogels.<sup>42,43</sup> Furthermore, GA hydrogels possess excellent therapeutic properties, including inherent anti-inflammatory and antibacterial effects.<sup>44–46</sup> Notley, GA's amphiphilic structure makes it an ideal candidate for drug delivery systems.<sup>47,48</sup> Thus, we present a novel wound dressing (GA/WS-CQDs) with synergistic and long-lasting therapy, which significantly promotes the healing of MRSA-infected wounds. Moreover, WS-CQDs released from the hydrogels demonstrate excellent anti-MRSA activity mainly via DNA damage and inhibition of bacteria biofilm formation. The GA/WS-CQDs dressings exhibit suitable mechanical strength properties for tissues, injectability, self-healing, excellent biocompatibility, sustained-release activity, efficient and lasting anti-MRSA and anti-inflammatory effects.

## Materials and Methods

### Materials

Tryptophan was supplied by Sigma-Aldrich (T2610000, St. Louis, MO, USA). Sorbitol was purchased from Aladdin Biochemical Technology Co., Ltd (S104834, Shanghai, China). Glycyrrhizic acid was supplied by Yuanye Biotechnology Co., Ltd (S24734, Shanghai, China). All test kits were commonly used in the laboratory.

### Bacterial Strains and Cells Culture

*S. aureus* (ATCC25923, ATCC29213), MRSA quality control bacteria (ATCC43300), MRSA clinical isolates (222,125,587, 223,116,824), *P. aeruginosa* (ATCC27853), and *E. coli* (ATCC25922) were provided by the Department of Clinical Laboratory in Xiangya Hospital of Central South University. Human umbilical vein endothelial cells (HUVECs) and Human skin fibroblasts (HDFs) were gifted by the Dermatology Department in Xiangya Hospital of Central South University.

### Preparation and Characterization of Hydrogels

0.001–0.06 g of GA powder was added to WS-CQDs solution. The mixtures were placed in a 60 °C water bath for 10 min to ensure that GA was completely dissolved. Afterwards, the mixed solution was naturally cooled at room temperature and finally the different concentrations of GA/WS-CQDs hydrogels were obtained. This facile process is dependent on self-assembly of GA hydrogels.<sup>42,49,50</sup> The GA hydrogels (GA-gel) and GA/WS-CQDs hydrogels (GA/WS-CQDs-gel) were lyophilized into powders. The micro-morphologies of the samples were observed using a scanning electron microscope (SEM; Quanta 250 FEG, FEI Corporation). Fourier transform infrared spectroscopy (FT-IR, PerkinElmer Spectrum Two, Llantrisant, UK) was performed on the samples in the 2000–400  $\text{cm}^{-1}$  range.

### Oscillatory Rheology Test

The rheological properties of GA/WS-CQDs-gel were analyzed by frequency, amplitude, viscosity sweep and continuous step strain tests using an MCR 302 rheometer (Anton Paar, Austria). The frequency ( $\omega$ ) sweep test was conducted at  $\omega = 0.1$ –100 rad/s with a fixed strain ( $\gamma$ ) of 0.5% at 25 °C. The strain amplitude sweep test was conducted at  $\gamma = 0.01$ –1000% with an oscillation frequency of 1 rad/s at 25 °C. The shear viscosity sweep test was conducted at  $\omega = 1$  rad/s with a fixed strain ( $\gamma$ ) of 0.5% at 25 °C, the rate of shear was enhanced from 0.1 to 100  $\text{s}^{-1}$  and then reduced from 100 to 0.1  $\text{s}^{-1}$ . The continuous step strain test was conducted at a fixed frequency of 1 rad/s at 25 °C, with a low strain of 0.1% for 120 s and a high strain of 100% for 12s. The continuous step strain test shall be conducted for at least three cycles.

## In vitro Sustained-Release Study

2 mL GA-gel or GA/WS-CQDs-gel (30 mg/mL) were prepared in a 5 mL glass. Then, added the 2 mL PBS (0.01 M, pH = 7.4) as a release solution and incubated at 37 °C with shaking (100 rpm/min). At predetermined time points (0, 2, 4, 8, 10, 20, 24, 36, 48, 60 h), the supernatant solutions (200 µL) were taken out. Meanwhile, the same volume of PBS was replenished into release system. Finally, the absorbance of the supernatant was measured at OD470 nm. According to the linear relationship between WS-CQDs concentration and the OD470 value, the cumulative release rate of WS-CQDs at the indicated time was calculated using the following equations:

$$\text{The cumulative amount of release (\%)} = V \times \sum_{m=1}^n \frac{C_m}{W} \times 100 \%$$

$C_m$  was the concentration of WS-CQDs in supernatant for each determination (µg/mL).  $V$  was the volume of each withdrawal sample (mL).  $W$  was the total amount of WS-CQDs additions (µg).

## Evaluation of antibacterial Activity in vitro

### Microdilution Standard Assay

Briefly, 10 µL of bacterial suspensions with a concentration of  $1 \times 10^7$  CFU mL<sup>-1</sup> were resuspended in 990 µL MH nutrient broth containing different concentrations of GA or WS-CQDs. Bacteria incubated with MH nutrient broth were utilized as negative control. MH nutrient broth with non-bacterial as a blank. After incubation for 12 h at 37 °C and 200 rpm, bacterial survival rates were determined by a microplate reader at OD600 nm.

### Standard Plate Counting Assay

The drugs treatment of bacteria is consistent with the above experiments. After incubation for 12 h at 37 °C and 200 rpm, the bacterial suspension was diluted 100,000-fold. Then, 60 µL diluted bacterial solution was added to LB agar plate. Incubate at 37 °C for 12 h and capture images of the clones.

### Inhibition-Zone Test

Overnight cultures of MRSA were diluted to a concentration of  $1 \times 10^4$  CFU mL<sup>-1</sup>. Soak the cotton swab and uniformly applied to the MH agar plate.  $14 \times 10 \times 6$  mm<sup>3</sup> penicillin hydrogels, vancomycin hydrogels, GA-gel, GA/WS-CQDs-gel were prepared and then placed on the plate. With reference to the antibiotic paper discs, the concentration of penicillin and vancomycin in hydrogel is 10 µg/mL. Incubate at 37 °C for 12 h, the inhibition-zone diameters of each well were measured.

### Checkerboard Synergy Technique

The antibacterial interaction was assessed using the checkerboard synergy technique with small modifications.<sup>51</sup> Serial 2-fold dilutions of WS-CQDs and GA were mixed in each well of a 96-well microtiter plate. Stock solutions of WS-CQDs and GA were diluted in an appropriate volume of MH broth. The concentrations of WS-CQDs ranged from 5 to 160 µg/mL, while GA concentrations ranged from 0.4 to 6.4 mg/mL. Well with only medium was used as control. The fractional inhibitory concentration index (FICI) explains the interaction between WS-CQDs and GA, which is calculated with the following equation:

$$\text{FIC of WS - CQDs} = \text{MIC of WS - CQDs in combination} / \text{MIC of WS - CQDs in alone}$$

$$\text{FIC of GA} = \text{MIC of GA in combination} / \text{MIC of GA in alone}$$

The FIC index (FICI) was calculated with the following formula:

$$\text{FICI} = \text{FIC of WS - CQDs} + \text{FIC of GA}$$

The results were interpreted as follows:  $\text{FICI} \leq 1$  is defined as synergy,  $2 \geq \text{FICI} \geq 1$ , additive,  $2 < \text{FICI} < 4$ , indifferent, while antagonism is considered when  $\text{FICI} \geq 4$  indicates antagonism.

## Calcein-AM/PI Assay

HUVECs and HDF cells were seeded into 24-well plates at a density of  $5 \times 10^4$  cells/well overnight, followed by incubation with the exudate of different GA/WS-CQDs-gel concentrations for 24 h. The preparation of hydrogels exudate was following: the sustained-release system was prepared and incubated at 37 °C with shaking (100 rpm/min), then the supernatant solutions (200  $\mu$ L) were taken out at predetermined time points (0, 12, 24, 48, 60 h). Meanwhile, the same volume of PBS was replenished into release system for next time. The collected supernatants were mixed together and diluted with culture medium. The medium-treated cells served as the control. Finally, cells were stained according to the calcein-AM/PI assay Kit instructions and observed by fluorescence microscope (Leica, DMi8). The dead (PI-positive) and live (calcein-AM-positive) cells appeared red and green fluorescence, respectively.

## In vivo Toxicity Evaluation

The whole blood, serum and organ tissues (liver, spleen, lung, kidney and heart) of the mice on 15th days after the topical application of GA/WS-CQDs-gel were harvested. Blood routine and biochemical test were conducted on automated instruments in the Department of Clinical Laboratory in Xiangya Hospital. The tissues were stained with hematoxylin-eosin (H&E) and the photographs of stained sections were taken by using an optical microscope (Leica, Germany).

## In vivo MRSA-Infected Wound Models and Treatments

BALB/c mice (8 weeks,  $22 \pm 0.5$  g) were purchased from Changzhou Cavens Laboratory Animal Company. Following 5 days acclimation, the full-thickness incision (5 mm diameter) in normal mice back after anesthesia with isoflurane were established. Then, 20  $\mu$ L of  $3.5 \times 10^8$  CFU  $\text{mL}^{-1}$  MRSA bacterial suspension was coated on the wounds. All mice were randomly divided into 3M film, GA dressing and GA/WS-CQDs dressing group. Observed wounds every day and recorded the healing time. Meanwhile, the mice were euthanized and the tissues of the wound skin were collected after the treatment 5 days. Then, the tissues of the wound skin were stained with immunohistochemistry (IHC), H&E and Masson's trichrome. The primary antibody TNF- $\alpha$  was 1:200 dilution (bs-2150R, Bioss), IL-1 $\beta$  was 1:200 dilution (16,806-1-AP, Proteintech) and IL-6 was 1:100 dilution (bs-6309r, Bioss). The photographs of stained sections were taken by using an optical microscope (Leica, Germany).

## Statistical Analysis

Statistical graphs were drawn by GraphPad Prism 8.0.1 or Origin software. Statistical analysis was performed by SPSS 20.0 software. Data were expressed as means  $\pm$  SD. Differences between the two groups were analyzed using Student's *t*-test or two-way ANOVA. Otherwise, comparisons were analyzed using nonparametric Mann-Whitney test.

Additional details regarding the methods were available in [Supplementary Material 1](#).

## Results and Discussion

### Preparation and Characterization of GA/WS-CQDs Hydrogels

In our design (Figure 1A), we prepared a biofriendly and transparent hydrogel by simply mixing GA powder and WS-CQDs solution. The hydrogel network formation is facilitated by hydrogen bond interactions between the hydroxyl and carboxyl groups of GA and the functional groups (hydroxyl, carboxyl, amino, indole) on the surfaces of WS-CQDs. Moreover,  $\pi$ - $\pi$  stacking between indole groups of WS-CQDs contributes to the formation of the GA/WS-CQDs-gel. The structure of GA/WS-CQDs-gel and GA-gel were characterized by Fourier transform infrared spectroscopy (FT-IR). As shown in Figure 1B, compared with the GA-gel, the peaks at  $1723 \text{ cm}^{-1}$  of the amide group and  $1698 \text{ cm}^{-1}$  of the carboxyl group were both sharply increased in the pattern of the GA-gel loaded with WS-CQDs, which attributed to the changes in hydrogen bond and non-covalent interactions. The 3D network skeleton formation of hydrogel with pore sizes of about 20–200 nm (Figure 1C) provides an irregular and uneven structure favorable for substance transmission and exchange when applied as wound dressings.<sup>52</sup> Compared to GA-gels, the GA/WS-CQDs-gels exhibited a relatively dense network structure, indicating that WS-CQDs increase the crosslinking density of the hydrogels.

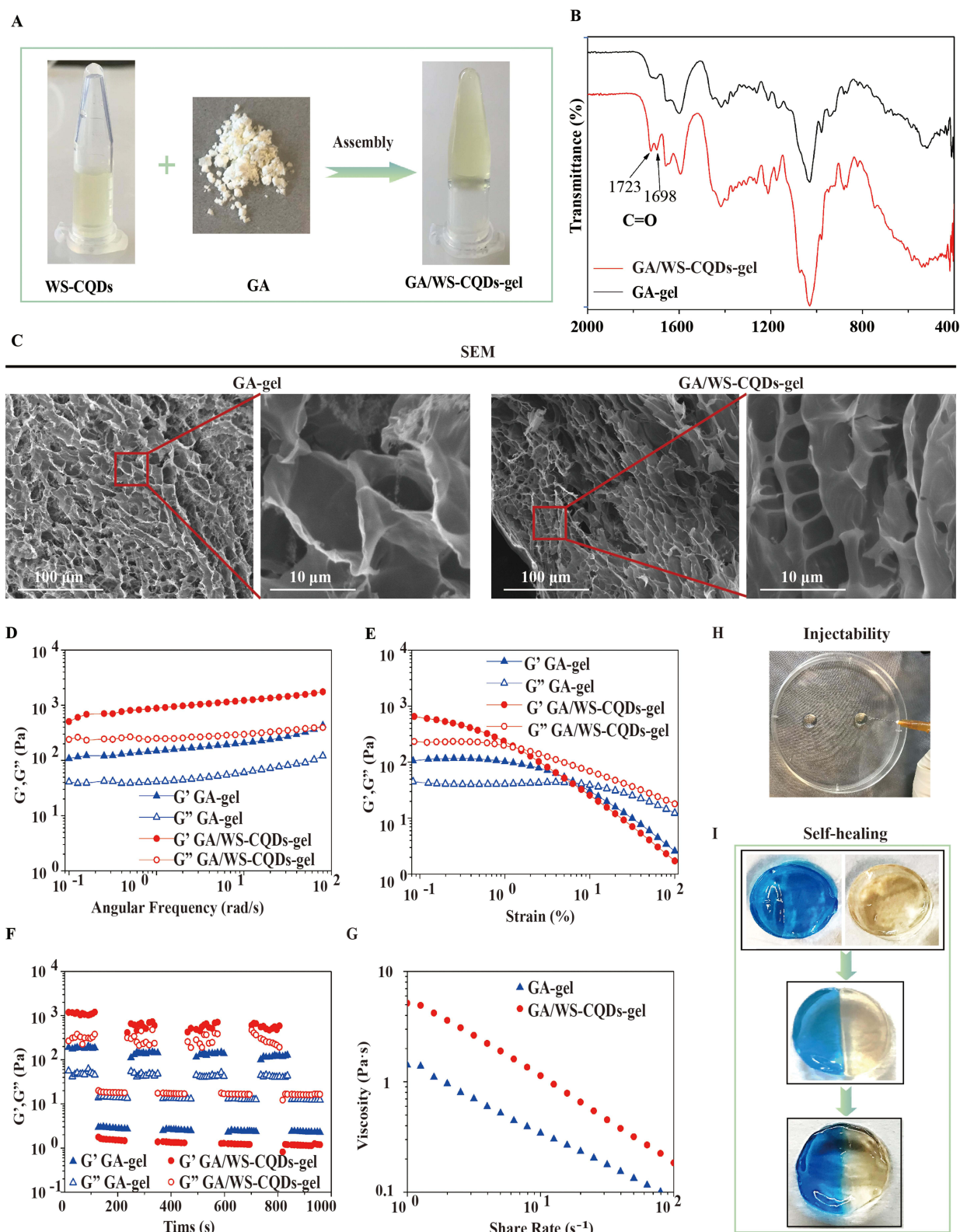


**Figure 1** Preparation of GA/WS-CQDs hydrogels. **(A)** The schematic diagram of the GA/WS-CQDs-gel preparation. **(B)** FT-IR characterization. **(C)** SEM images of the GA-gel and GA/WS-CQDs-gel. **(D–G)** Rheology test of the GA-gel and GA/WS-CQDs-gel. Frequency scan **(D)**, Amplitude scan **(E)**, Cycle scan **(F)**, Complex viscosity scan **(G)**. **(H)** Schematic of GA/WS-CQDs-gel injectability. **(I)** Self-healing process of GA/WS-CQDs-gel after cutting.

The rheological characteristics, such as mechanical strength, flow behavior, and viscoelasticity, are crucial for the application and transformation of hydrogel materials.<sup>53</sup> The elastic behavior of the GA-gel and GA/WS-CQDs-gel was confirmed by the storage modulus ( $G'$ ) consistently larger than the loss modulus ( $G''$ ) (Figure 1D). The GA/WS-CQDs-gel exhibited a higher mechanical strength, as evidenced by the destruction of the network structure at a lower strain ( $\gamma = 50\%$ ) compared to the GA gel ( $\gamma = 200\%$ ) (Figure 1E). Both the GA-gel and GA/WS-CQDs-gel demonstrated good self-healing, as they could return to the hydrogel state well after three transitions from high to low strain (Figure 1F). The shear thinning behavior observed in Figure 1G indicated injectability of the hydrogels. The good self-healing and injectable properties of the GA/WS-CQDs gel were further confirmed (Figure 1H and I). These features make GA/WS-CQDs hydrogels an ideal choice for wound dressings.

## The Remarkable Anti-MRSA Synergism Between WS-CQDs and GA

WS-CQDs possess ultrasmall size, high water-solubility, good stability, multicolor fluorescence emission (Supplementary Figure 1), outstanding biocompatibility (Supplementary Figure 2), and excellent anti-MRSA activity with low drug resistance (Supplementary Table 1 and Supplementary Figure 3). The anti-MRSA activity of the different combination between GA and WS-CQDs was tested, and heat maps were used to visually display the OD values obtained from bacterial growth inhibition assays (Figure 2A and B). The results confirmed the excellent anti-MRSA activity of both GA

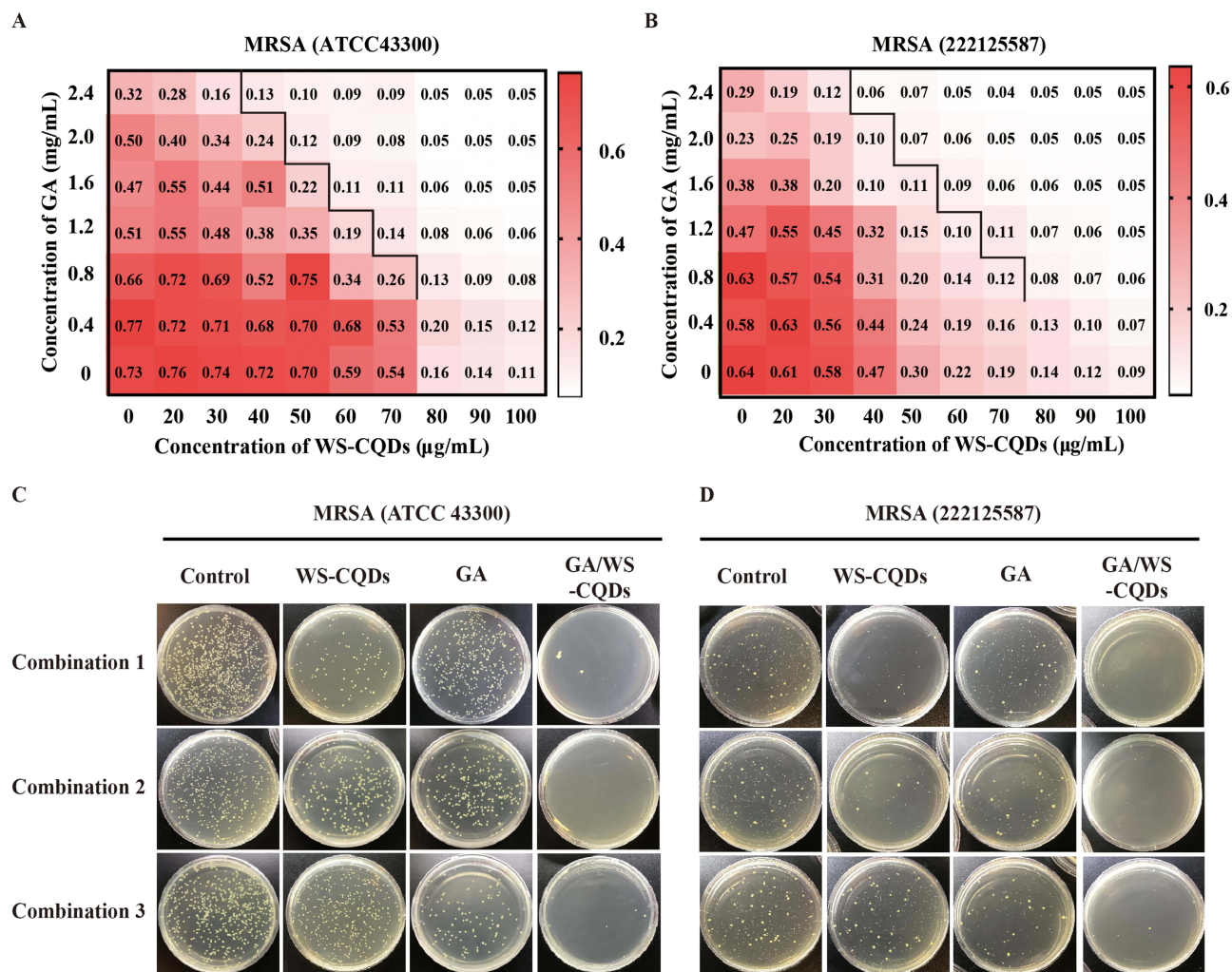


**Figure 2** The noticeable anti-MRSA synergism between WS-CQDs and GA. (A and B) Heat map visually displayed the growth inhibition of bacterial treated with different combination between WS-CQDs and GA. The numbers in the heat map are the corresponding OD values. (C and D) Standard plate counting method, the representative digital images of agar plates displaying results for WS-CQDs, GA, GA/WS-CQDs and PBS (control group) against MRSA. Combination 1 (low concentration of GA and high concentration of WS-CQDs), combinations 2 ( $1/2 \times$  MICs of GA and  $1/2 \times$  MICs of WS-CQDs), and combinations 3 (high concentration of GA and low concentration of WS-CQDs).

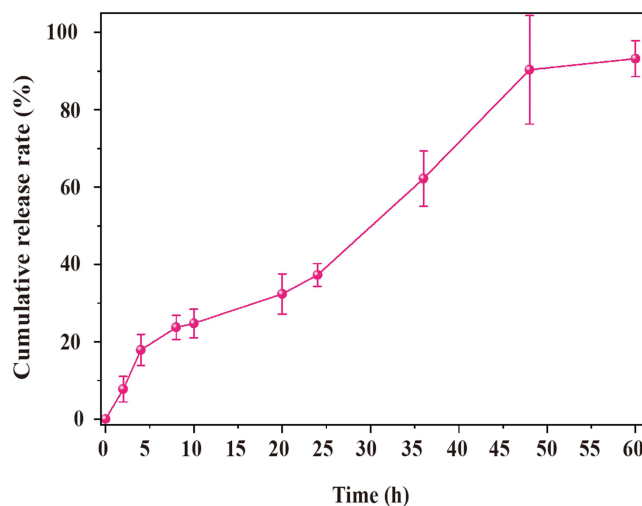
**Table 1** The Synergistic Interaction of Combined WS-CQDs with GA Against MRSA

Antibacterial Agents	MICs		FIC	FICI	Interaction
	Alone	Combination			
WS-CQDs ( $\mu\text{g/mL}$ )	80	40	0.5	0.75	Synergy
GA-gel (mg/mL)	6.4	1.6	0.25		

and WS-CQDs individually and indicated different combinations for efficient eradication of MRSA bacteria. Three combinations were selected for further evaluation using the standard plate counting method (Figure 2C and D). The GA/WS-CQDs-gel exhibited the minimum number of MRSA clones among the three combinations, indicating the strongest anti-MRSA activity. The fractional inhibitory concentration index (FICI) value of 0.75 ( $< 1$ ) confirmed the remarkable anti-MRSA synergism between WS-CQDs and GA (Table 1). These results support the use of GA/WS-CQDs-gel wound dressing as an effective strategy for eradicating MRSA bacteria due to their noticeable anti-MRSA synergism.

### In vitro Sustained-Release Behavior of GA/WS-CQDs Hydrogels

The release of therapeutics from hydrogels can be controlled by various features such as size, shape, architecture, and physical/chemical cross-linking.<sup>54</sup> To observe the release behavior of GA/WS-CQDs hydrogels at the phosphate buffer solution (0.01 M, pH 7.4), we conducted in vitro experiments using Microplate Reader. The OD470 value exhibited a linear relationship with the concentration of WS-CQD (Supplementary Figure 4). As illustrated in Figure 3, the GA/WS-CQDs hydrogels released WS-CQDs quickly during the first 4 h, followed by a gradual release process. However, WS-CQDs began to release rapidly again after 20 h, although at slightly lower rate than the initial 4 h. The release of WS-CQDs from GA/WS-CQDs hydrogels continued for up to 60 h, with the cumulative release over 90%. Based on release kinetics,<sup>45</sup> this sustained-release behavior at stage I (0–20 h) and stage II (20–60 h) followed a first-order release pattern, revealing that WS-CQDs mainly released through diffusion from the hydrophilic channel of GA hydrogels. GA hydrogels is self-assembly (Supplementary Figure 5 and 6), which contributed to this sustained-release behavior. These results demonstrate that GA/WS-CQDs hydrogels can achieve long-lasting release of WS-CQDs at wound sites, thereby extending the half-life of drugs, reducing the frequency of administration, and minimizing the number of dressing changes required.

**Figure 3** In vitro the cumulative release curves of WS-CQDs from the GA/WS-CQDs hydrogel.

## In vitro Anti-MRSA Activity and Biocompatibility of GA/WS-CQDs Hydrogels

The anti-MRSA effect of GA/WS-CQDs hydrogels were determined using the modified Oxford cup method.<sup>55</sup> As shown in [Figure 4](#), the inhibition-zone diameter of GA/WS-CQDs hydrogels against MRSA was significantly larger than that of common antibiotics such as penicillin, vancomycin, as well as GA hydrogels. Notably, MRSA bacteria are resistance to penicillin, which served as a negative control. Currently, vancomycin is the first-line approved agent for treating MRSA infection,<sup>56</sup> but its use in the clinic is associated with cytopenia, ototoxicity, and nephrotoxicity, necessitating caution.<sup>57</sup> These findings indicate the promising prospect of GA/WS-CQDs hydrogels as a highly potent anti-MRSA material surpassing the efficacy of vancomycin and GA hydrogels, making significant progress in the management of infected wounds.

Biocompatibility is a crucial consideration for biomaterials used in clinical applications. In order to assess the cytotoxicity of GA/WS-CQDs hydrogels materials in vitro, we cultured cells with the hydrogel exudate and performed calcein-AM/PI assay. The results ([Figure 5A](#)) showed the GA/WS-CQDs hydrogels exhibited no cytotoxicity for HUVECs and HDF cells when compared to the control group, with almost 100% of cells showing green fluorescence (indicating live cells). The hemolysis rate of 60 mg/mL hydrogels exudate was calculated to be only 2.79% (< 5%), indicating good blood compatibility of GA/WS-CQDs hydrogels within the effective antibacterial concentration range ([Figure 5B](#)). Furthermore, GA/WS-CQDs dressings had no obvious toxicity in BALB/c mice after 15 days of application ([Figure 5C and D](#)). While Ag<sup>+</sup>-containing hydrogels have been used as wound dressings in clinic for their excellent antibacterial effect, their clinical applications are limited due to significantly toxicity associated with heavy metals. Additionally, their degradation curves observed in vitro experiments were shown in [Supplementary Figure 7](#). Based on these results, GA/WS-CQDs dressings demonstrate excellent biocompatibility with minimal toxicity and good degradability, making them highly suitable for medical applications.

## GA/WS-CQDs Dressings for MRSA-Infected Wounds in vivo

In comparison to conventional hydrogel wound dressings, our design ([Figure 6A](#)) involved placing GA/WS-CQDs hydrogels on 3M film to prepare the GA/WS-CQDs dressings, which are bio-friendly, low-cost, and hold great potential for clinical translation. To evaluate the therapeutic potential of GA/WS-CQDs dressings for treating MRSA-infected wounds in vivo, we utilized an MRSA-infected full-thickness incision mice model ([Figure 6B](#)). The experimental protocol involved dividing the mice randomly into three groups: 3M film, GA dressing, and GA/WS-CQDs dressing. The commercial 3M film was used as the control group and no dressings changes were required throughout the entire experiment. The hydrogels can thoroughly spread over mouse wounds ([Supplementary Figure 8](#)) and be completely absorbed or degraded within 72 h after treatment

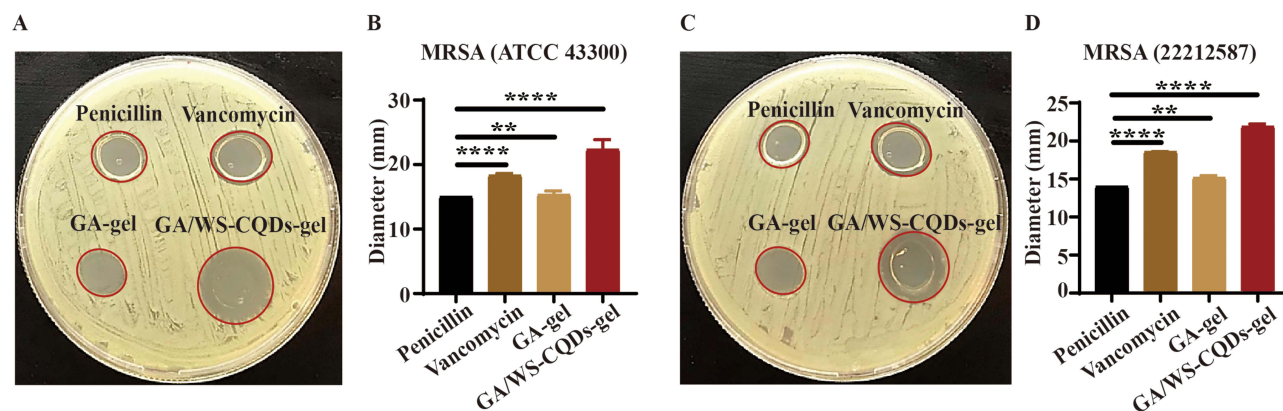


**Figure 4** The anti-MRSA activity of GA/WS-CQDs hydrogels. Inhibition-zone test for 10  $\mu$ g/mL penicillin hydrogels, 10  $\mu$ g/mL vancomycin hydrogels, GA-gel, and GA/WS-CQDs-gel against MRSA, (A) Representative digital images and (B) statistical analysis showed antibacterial capacity by inhibition-zone test against MRSA (ATCC 43300). (C) Representative digital images and (D) statistical analysis against MRSA (22,212,587). The data are mean  $\pm$  SD ( $n=3$ , statistical significance was analyzed via unpaired t-test, \*\* $p < 0.01$ , \*\*\* $p < 0.001$ ).

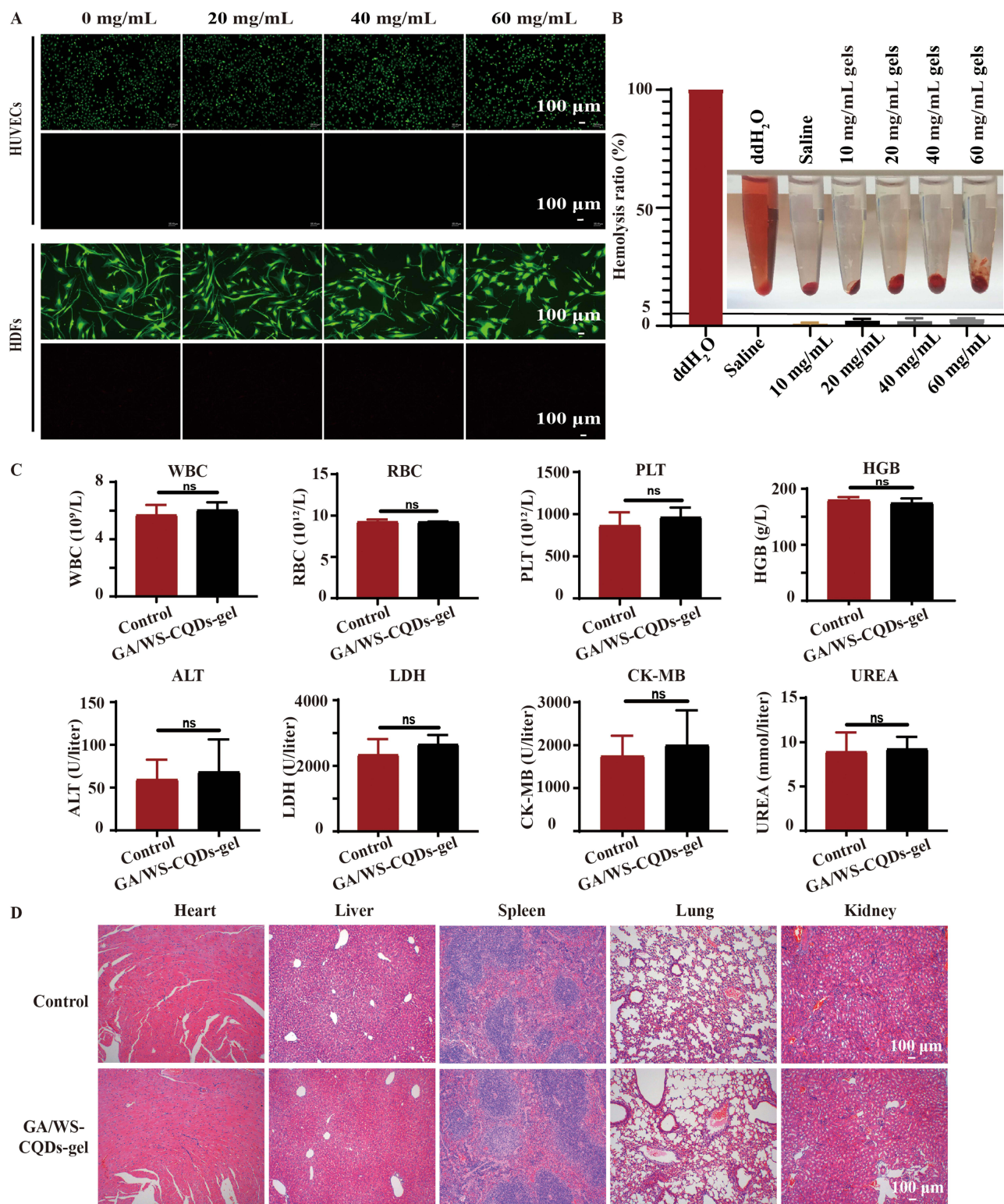


**Figure 5** The biosafety assessment of GA/WS-CQDs hydrogels in vitro and in vivo. **(A)** Calcein-AM/PI staining images of cells treated with the exudate of different concentrations hydrogels for 24 h. Green fluorescence (live cells), red fluorescence (death cells). **(B)** Hemolysis assay. Saline and ddH<sub>2</sub>O as negative and positive control group, respectively. **(C)** The change of white blood cells (WBC), red blood cells (RBC), platelets (PLT), hemoglobin (HGB), ALT (*alanine aminotransferase*), LDH (*lactate dehydrogenase*), CK-MB (*creatin kinase MB*), UREA. ns represents not significant. **(D)** H&E staining images of heart, liver, spleen, lung, and kidney sections from mice with wounds. Scale bar, 100  $\mu$ m.

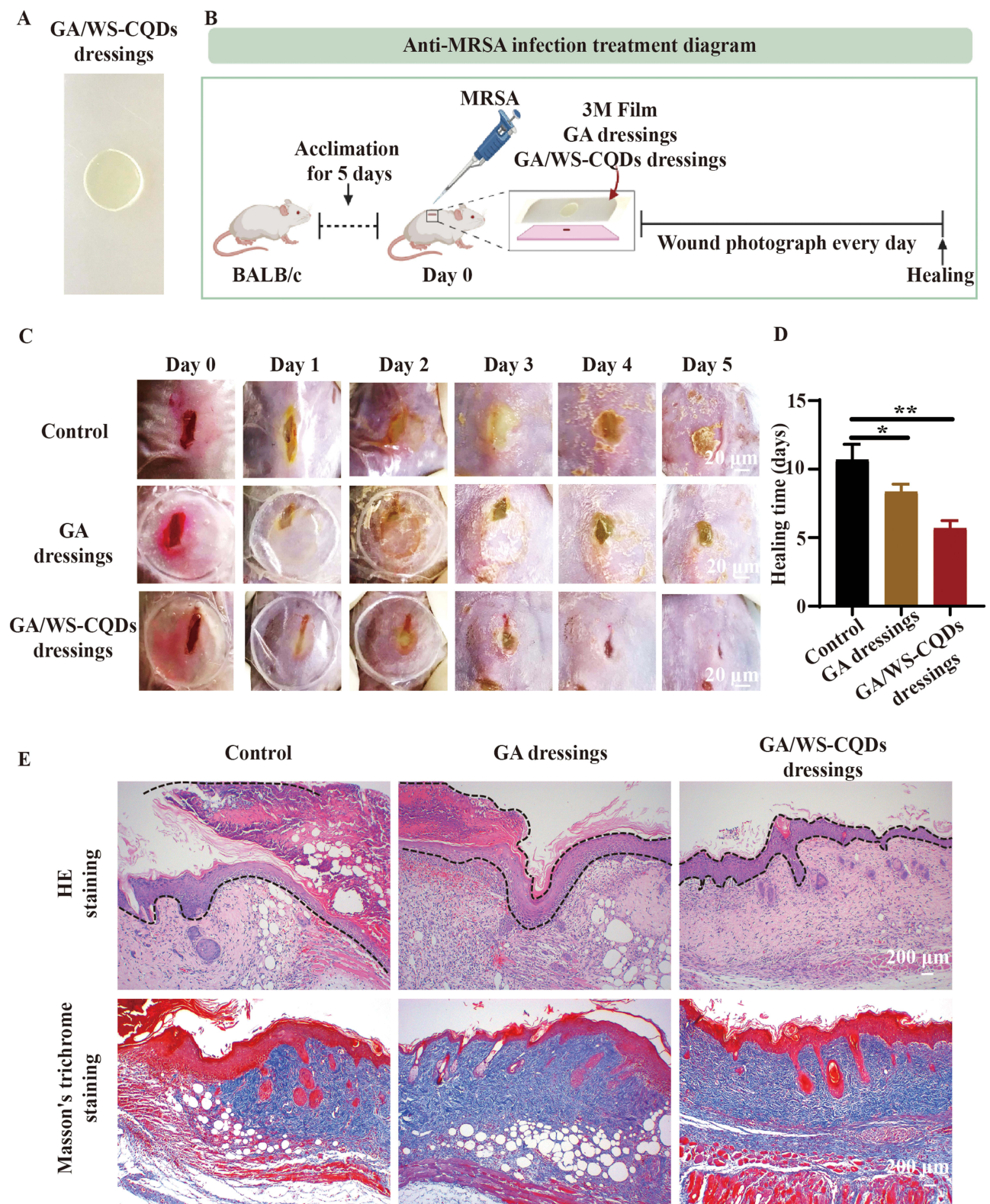


**Figure 6** GA/WS-CQDs dressings accelerated MRSA-infected wounds healing in vivo. **(A)** Image of GA/WS-CQDs dressings. **(B)** Pattern diagram of MRSA-infected wound model and treatment. **(C)** Representative images of wounds treated with 3M film, GA dressings, and GA/WS-CQDs dressings at the indicated time points. Scale bar, 20  $\mu$ m. **(D)** Statistical of the healing times in every group.  $**p < 0.01$ ,  $*p < 0.05$ . **(E)** H&E and Masson's trichrome staining of wounds skin tissue. Black dashed line, epidermis. Scale bar, 200  $\mu$ m.

([Supplementary Figure 9](#)). It was found that the wounds treated with 3M film exhibited suppuration and were filled with massive abscess, whereas the wounds treated with GA dressings and GA/WS-CQDs dressings showed gradual regeneration. After 5 days of treatment, the wounds treated with GA/WS-CQDs dressings demonstrated significant progress towards complete healing, while the GA dressings group exhibited slow wound healing ([Figure 6C](#)). Overall, GA/WS-CQDs dressings significantly shorten the healing time compared to the 3M film and GA dressing group ([Figure 6D](#)). H&E staining showed that the epidermis structure of control and GA dressing groups were incomplete and significantly thickened significantly, whereas the GA/WS-CQDs dressings groups exhibited well-organized lamellar epithelium, orderly granulation tissue, blood vessels and hair follicles. Mason's trichrome staining showed the collagen fiber deposition areas of the control, GA dressings, and GA/WS-CQDs dressings groups were 13.3%, 46.7% and 51%, respectively ([Figure 6E](#)). Immunohistochemistry revealed TNF- $\alpha$ , IL-1 $\beta$ , and IL-6 were lower expression in GA/WS-CQDs dressings group ([Figure 7A and B](#)). Additionally, GA/WS-CQDs hydrogels led to a significant increase in the wound healing area in an MRSA-infected full-thickness skin mice model ([Supplementary Figure 10](#)). Collectively, GA/WS-CQDs dressings demonstrated considerable therapeutic efficacy in treating MRSA-infected wounds in vivo.

## The Antibacterial Mechanism of WS-CQDs

In order to better understand how the GA/WS-CQDs-gel plays an anti-MRSA synergy, it was necessary to investigate the antibacterial mechanism of WS-CQDs. As shown in [Supplementary Figure 11](#), WS-CQDs with positive charge actively entered bacteria, and internalization of WS-CQDs was the primary condition for exerting antibacterial ability. Transcriptome sequence analysis was conducted to investigate its potential antibacterial mechanism. The Gene Ontology (GO) database showed significant changes in bacteria molecular function upon exposure to WS-CQDs, with most differentially expressed proteins (DEPs) being related to nucleic acid and DNA binding ([Figure 8A](#)). Nucleic acid is not only essential for protein biosynthesis, but also serves as the material basis of biological function.<sup>58</sup> It is widely accepted that endocytosed nanomaterials directly or indirectly interfere with DNA replication to achieve antibacterial effects.<sup>59,60</sup> To assess the possibility of DNA damage, the electrophoretic mobility of DNA bands was analyzed. Overall, the damage degree of DNA framework in *S. aureus* and MRSA treated with WS-CQDs was similar ([Figure 8B](#)). The electrophoresis pattern clearly showed a bright and compact DNA band (Lane 1) for control group, whereas almost no DNA bands were observed when the concentration ratios of DNA to WS-CQDs was 1: 0.6 (Lane 3). Furthermore, transmission electron microscope also observed the change of chromatin, the heterogeneous division, and the breakage of cell wall and membrane ([Supplementary Figure 12](#)). These results indicated that WS-CQDs could directly damage DNA framework against *S. aureus* and MRSA.

Moreover, the Kyoto Encyclopedia of Genes and Genome (KEGG) database identified the enrichment of the first two pathways, including ABC transporters and two-component system ([Figure 8C](#)). Both systems have demonstrated their ability in drug antibiotic transport and resistance.<sup>61</sup> Previous reports have shown that 80% of bacterial infections and drug resistance are associated with bacterial biofilms formation.<sup>1</sup> As shown in [Figure 8D and E](#), WS-CQDs effectively inhibited the biofilm formation of *S. aureus* and MRSA, which is conducive to reducing the risk of drug resistance.

The anti-MRSA mechanisms of GA mainly involve the down-regulation of virulence genes, the inhibition of  $\alpha$ -hemolysin production, and anti-biofilm formation.<sup>43,62,63</sup> GA derivative hydrogels initially adhere to the surface and enter the bacteria, then affect arginine biosynthesis and metabolism, ultimately leading to bacteria death.<sup>64,65</sup> Thus, we propose that the highly effective anti-MRSA of GA/WS-CQDs hydrogels possibly operates following three aspects. (a) sustained-released WS-CQDs that translocate into bacteria via electrostatic attraction, directly damaging bacterial DNA and affecting related gene expression, leading to bacterial death, (b) both GA and WS-CQDs inhibit the formation of bacteria biofilms, and (c) GA adheres to the surface of the bacteria, enters the bacteria, then downregulates the virulence genes and metabolism-related genes of MRSA, leading to bacterial death. However, the detail mechanisms require further exploration.

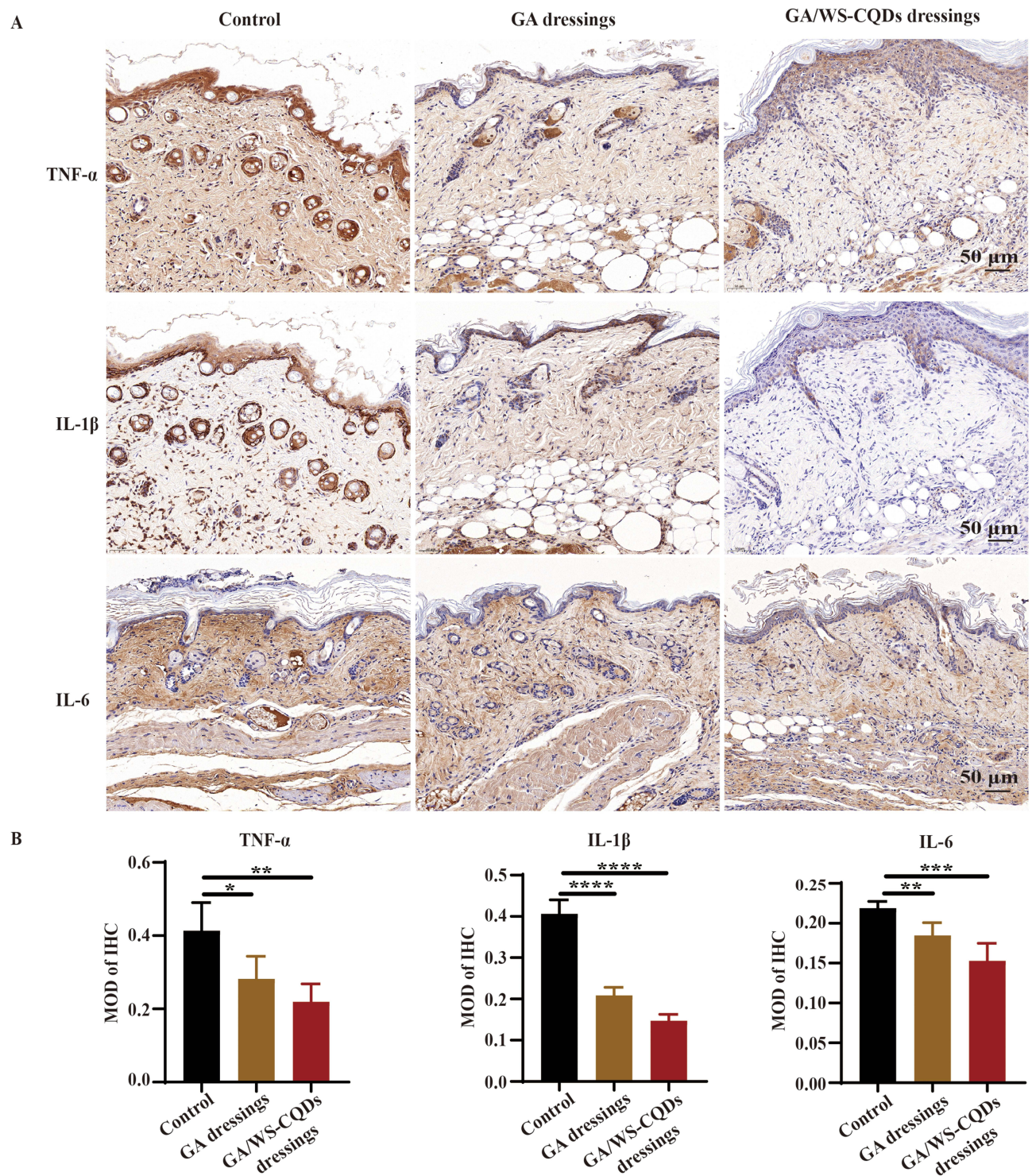


**Figure 7** GA/WS-CQDs dressing inhibited wound inflammation in vivo. **(A)** Immunohistochemical staining images of proinflammatory factors including TNF- $\alpha$ , IL-1 $\beta$  and IL-6 in MRSA-infected wound skin tissues. Scale bar, 50  $\mu$ m. **(B)** Quantification of the mean intensities for the areas positive from **(A)**. \*\*\*\* $p$  < 0.001, \*\*\* $p$  < 0.005, \*\* $p$  < 0.01, and \* $p$  < 0.05.

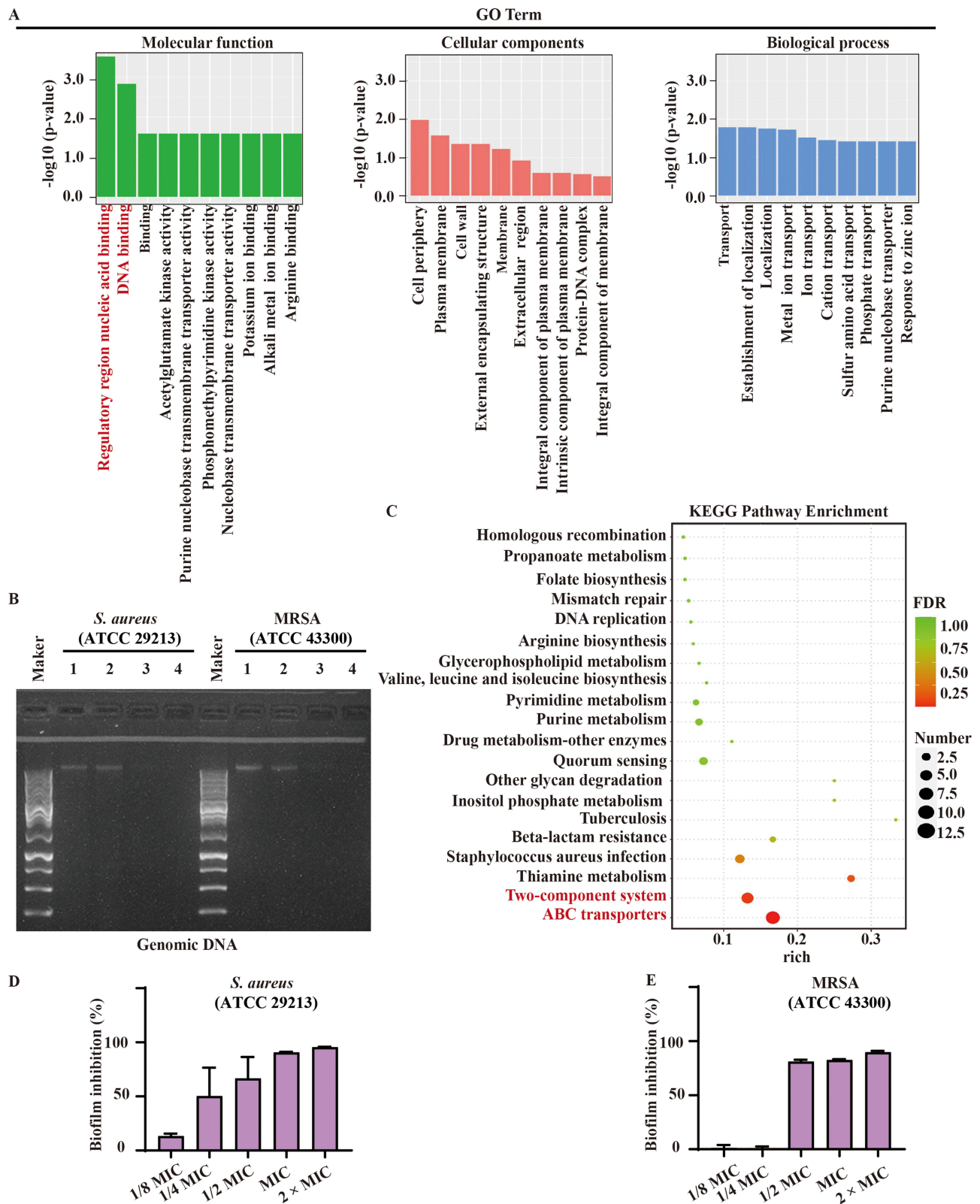


**Figure 8** The antibacterial mechanism of WS-CQDs. RNA-Seq gene expression profiles. Control vs WS-CQDs treated groups. Red text indicates gene or pathways with the most significant differential expression. **(A)** Go enrichment analysis in molecular function (MF), cellular component (CC) and biological process (BP). **(B)** Gel electrophoretic mobility of WS-CQDs binding to bacteria genomic DNA. Band 1 (control), band 2 (1:0.3), band 3 (1:0.6) and band 4 (1:1.2). **(C)** KEGG enrichment analysis. **(D and E)** Inhibition rates of the biofilm formation of *S. aureus* and MRSA.

## Conclusions

In conclusion, we have presented the design principles of biocompatible wound dressings that combine the structural and functional characteristics of WS-CQDs and GA hydrogels to achieve synergistic and long-lasting anti-MRSA and anti-inflammatory effects. The mechanical performance and compatibility with cells and tissues make GA/WS-CQDs dressings meet the key requirements for next-generation wound dressings. The most remarkable feature of GA/WS-CQDs dressings are their simple preparation, visual monitoring, biodegradability, significant anti-MRSA synergism, and long-lasting release properties, making a breakthrough in bacteria-infected wound care management. In addition, in vivo experiments have confirmed that the GA/WS-CQDs dressings reduce the expression of inflammatory factors (TNF- $\alpha$ , IL-1 $\beta$ , and IL-6) and significantly promote MRSA-infected wound healing without causing systemic toxicity. This study highlights the highly promising potential of GA/WS-CQDs dressings for treating MRSA-infected wound healing in clinical settings.

## Acknowledgments

This study was supported by the National Natural Science Foundation of China (No. 82270633), Hunan Provincial Natural Science Foundation of China (No. 2022JJ70076 and 2022JJ40840), and Clinical Research Center Foundation of Xiangya Hospital (No. LN2021XYSX).

## Ethics Approval and Consent to Participate

Animal experiments were approved by the Ethical Committee of Xiangya Hospital, Central South University in accordance with the guide for the Care and Use of Laboratory Animals in the “Regulations for the Administration of Experimental Animals” and “Measures for the Administration of Experimental Animals in Hunan Province”. And the Ethical approval number is 202103401. The human cell lines were approved by the Ethical Committee of Xiangya Hospital, Central South University. The collection and use of human cells complied with national regulations and Xiangya hospital research administration policies, as well as the Ethical approval number is 201403146.

## Disclosure

Dr Xiangjie Fu reports a patent CN202211567680.6. The authors declare that they have no other competing interests.

## References

1. Ouyang J, Bu QY, Tao N, et al. A facile and general method for synthesis of antibiotic-free protein-based hydrogel: wound dressing for the eradication of drug-resistant bacteria and biofilms. *Bioact Mater*. 2022;18446–18458. doi:10.1016/j.bioactmat.2022.03.033
2. Hassoun A, Linden PK, Friedman B, Sinderby C, Rozé H, Brochard L. Incidence, prevalence, and management of MRSA bacteremia across patient populations—a review of recent developments in MRSA management and treatment. *Crit Care*. 2017;21:21. doi:10.1186/s13054-017-1801-3
3. Brown ED, Wright GD. Antibacterial drug discovery in the resistance era. *Nature*. 2016;529(7586):336–343. doi:10.1038/nature17042
4. Sanabria-Rios DJ, Alequin-Torres D, De Jesus A, Cortes G, Carballeira NM. Vinyl halogenated fatty acids display antibacterial activity against clinical isolates of methicillin-resistant *Staphylococcus aureus*. *Med Res Arch*. 2022;10(7). doi:10.18103/mra.v10i7.2901
5. Yao G, Mo X, Yin C, et al. A programmable and skin temperature-activated electromechanical synergistic dressing for effective wound healing. *Sci Adv*. 2022;8(4):eabl8379. doi:10.1126/sciadv.abl8379
6. Zhao Q, Liu J, Liu SH, et al. Multipronged micelles-hydrogel for targeted and prolonged drug delivery in chronic wound infections. *ACS Appl Mater Inter*. 2022. doi:10.1021/acsami.2c12530
7. Simonetti O, Marasca S, Candelora M, et al. Methicillin-resistant *Staphylococcus aureus* as a cause of chronic wound infections: alternative strategies for management. *Aims Microbiol*. 2022;8(2):125–137. doi:10.3934/microbiol.2022011
8. Ali Alghamdi B, Al-Johani I, Al-Shamrani JM, et al. Antimicrobial resistance in methicillin-resistant *Staphylococcus aureus*. *Saudi J Biol Sci*. 2023;30(4):103604. doi:10.1016/j.sjbs.2023.103604
9. Nandhini P, Gupta PK, Mahapatra AK, et al. In-Silico molecular screening of natural compounds as a potential therapeutic inhibitor for methicillin-resistant *Staphylococcus aureus* inhibition. *Chem Biol Interact*. 2023;374:110383. doi:10.1016/j.cbi.2023.110383
10. Luneva O, Olekhovich R, Uspenskaya M. Bilayer hydrogels for wound dressing and tissue engineering. *Polymers*. 2022;14(15):3135. doi:10.3390/polym14153135
11. Yao H, Wu M, Lin LW, et al. Design strategies for adhesive hydrogels with natural antibacterial agents as wound dressings: status and trends. *Mater Today Bio*. 2022;16. doi:10.1016/j.mtbio.2022.100429
12. Liu J, Jiang WQ, Xu QY, Zheng YJ. Progress in antibacterial hydrogel dressing. *Gels-Basel*. 2022;8(8). doi:10.3390/gels8080503
13. Solanki D, Vinchhi P, Patel MM. Design considerations, formulation approaches, and strategic advances of hydrogel dressings for chronic wound management. *ACS Omega*. 2023;8(9):8172–8189. doi:10.1021/acsomega.2c06806

14. Cao H, Duan L, Zhang Y, Cao J, Zhang K. Current hydrogel advances in physicochemical and biological response-driven biomedical application diversity. *Signal Transduct Target Ther.* 2021;6(1):426. doi:10.1038/s41392-021-00830-x
15. Khan MUA, Stojanovic GM, Hassan R, Anand TJS, Al-Ejji M, Hasan A. Role of graphene oxide in bacterial cellulose-gelatin hydrogels for wound dressing applications. *ACS Omega.* 2023;8(18):15909–15919. doi:10.1021/acsomega.2c07279
16. Long L, Liu W, Hu C, Yang L, Wang Y. Construction of multifunctional wound dressings with their application in chronic wound treatment. *Biomater Sci.* 2022;10(15):4058–4076. doi:10.1039/d2bm00620k
17. Zmejkoski DZ, Markovici ZM, Mitic DD, et al. Antibacterial composite hydrogels of graphene quantum dots and bacterial cellulose accelerate wound healing. *J Biomed Mater Res B.* 2022;110(8):1796–1805. doi:10.1002/jbm.b.35037
18. Shen Z, Zhang C, Wang T, Xu J. Advances in functional hydrogel wound dressings: a review. *Polymers.* 2023;15(9):2000. doi:10.3390/polym15092000
19. Li S, Dong S, Xu W, et al. Antibacterial Hydrogels. *Adv Sci.* 2018;5(5):1700527. doi:10.1002/advs.201700527
20. Yang K, Zhou XY, Li ZL, Wang ZF, Deng L, He DG. Ultrastretchable, self-healable, and tissue-adhesive hydrogel dressings involving nanoscale tannic acid/ferric ion complexes for combating bacterial infection and promoting wound healing. *ACS Appl Mater Inter.* 2022. doi:10.1021/acsomega.2c13283
21. Wang Y, Lv T, Yin K, et al. Carbon dot-based hydrogels: preparations, properties, and applications. *Small.* 2023;19:e2207048. doi:10.1002/sml.202207048
22. Wan JF, Zhang XY, Fu K, Zhang X, Shang L, Su ZQ. Highly fluorescent carbon dots as novel theranostic agents for biomedical applications. *Nanoscale.* 2021;13(41):17236–17253. doi:10.1039/d1nr03740d
23. Sabzehmeidani MM, Kazemzad M. Quantum dots based sensitive nanosensors for detection of antibiotics in natural products: a review. *Sci Total Environ.* 2022;810. doi:10.1016/j.scitotenv.2021.151997
24. Sadat Z, Farrokhi-Hajjiabad F, Lalebeigi F, et al. A comprehensive review on the applications of carbon-based nanostructures in wound healing: from antibacterial aspects to cell growth stimulation. *Biomater Sci.* 2022;10:6911–6938. doi:10.1039/d2bm01308h
25. Zhao CF, Wang XW, Yu LY, et al. Quaternized carbon quantum dots with broad-spectrum antibacterial activity for the treatment of wounds infected with mixed bacteria. *Acta Biomater.* 2022;138528–138544. doi:10.1016/j.actbio.2021.11.010
26. Wu YY, Li C, van der Mei HC, Busscher HJ, Ren YJ. Carbon quantum dots derived from different carbon sources for antibacterial applications. *Antibiotics-Basel.* 2021;10(6). doi:10.3390/antibiotics10060623
27. Zhao D, Zhang R, Liu XM, Huang XJ, Xiao XC, Yuan L. One-step synthesis of blue-green luminescent carbon dots by a low-temperature rapid method and their high-performance antibacterial effect and bacterial imaging. *Nanotechnology.* 2021;32(15):155101. doi:10.1088/1361-6528/abd8b0
28. Yue J, Miao P, Li L, Yan R, Dong WF, Mei Q. Injectable carbon dots-based hydrogel for combined photothermal therapy and photodynamic therapy of cancer. *ACS Appl Mater Interfaces.* 2022;14:49582–49591. doi:10.1021/acsomega.2c15428
29. Campea MA, Majcher MJ, Lofts A, Hoare T. A review of design and fabrication methods for nanoparticle network hydrogels for biomedical, environmental, and industrial applications. *Adv Funct Mater.* 2021;31(33):2102355. doi:10.1002/adfm.202102355
30. Patel DK, Ganguly K, Jin HX, Dutta SD, Patil TV, Lim KT. Functionalized chitosan/spherical nanocellulose-based hydrogel with superior antibacterial efficiency for wound healing. *Carbohydr Polym.* 2022;284. doi:10.1016/j.carbpol.2022.119202
31. Stoica AE, Chircov C, Grumezescu AM. Nanomaterials for wound dressings: an up-to-date overview. *Molecules.* 2020;25(11):2699. doi:10.3390/molecules25112699
32. Kazeminava F, Javanbakht S, Nouri M, et al. Gentamicin-loaded chitosan/folic acid-based carbon quantum dots nanocomposite hydrogel films as potential antimicrobial wound dressing. *J Biol Eng.* 2022;16(1):36. doi:10.1186/s13036-022-00318-4
33. Moniruzzaman M, Dutta SD, Hexiu J, et al. Polyphenol derived bioactive carbon quantum dot-incorporated multifunctional hydrogels as an oxidative stress attenuator for antiaging and in vivo wound-healing applications. *Biomater Sci.* 2022;10(13):3527–3539. doi:10.1039/d2bm00424k
34. Cui F, Sun J, Ji J, Yang X. Carbon dots-releasing hydrogels with antibacterial activity, high biocompatibility, and fluorescence performance as candidate materials for wound healing. *J Hazard Mater.* 2021;406124330. doi:10.1016/j.jhazmat.2020.124330
35. Wang Y, Chen J, Tian JK, et al. Tryptophan-sorbitol based carbon quantum dots for theranostics against hepatocellular carcinoma. *J Nanobiotechnol.* 2022;20(1). doi:10.1186/s12951-022-01275-2
36. Cui FC, Sun JD, Ji J, et al. Carbon dots-releasing hydrogels with antibacterial activity, high biocompatibility, and fluorescence performance as candidate materials for wound healing. *J Hazard Mater.* 2021;406. doi:10.1016/j.jhazmat.2020.124330
37. Yang X, Li PL, Tang WT, et al. A facile injectable carbon dot/oxidative polysaccharide hydrogel with potent self-healing and high antibacterial activity. *Carbohydr Polym.* 2021;251. doi:10.1016/j.carbpol.2020.117040
38. Stenlund P, Enstedt L, Gilljam KM, et al. Development of an all-marine 3D printed bioactive hydrogel dressing for treatment of hard-to-heal wounds. *Polymers.* 2023;15(12):2627. doi:10.3390/polym15122627
39. Cao ZM, Luo Y, Li ZY, et al. Antibacterial Hybrid Hydrogels. *Macromol Biosci.* 2021;21(1):2000252. doi:10.1002/mabi.202000252
40. Trombino S, Sole R, Curcio F, Cassano R. Polymeric based hydrogel membranes for biomedical applications. *Membranes.* 2023;13(6). doi:10.3390/membranes13060576
41. Guo M, Wang Y, Gao B, He B. Shark tooth-inspired microneedle dressing for intelligent wound management. *ACS Nano.* 2021;15(9):15316–15327. doi:10.1021/acsnano.1c06279
42. Li Q, Zhang S, Du R, et al. Injectable self-healing adhesive natural glycyrrhizic acid bioactive hydrogel for bacteria-infected wound healing. *ACS Appl Mater Interfaces.* 2023;15(14):17562–17576. doi:10.1021/acsomega.2c23231
43. Rohinishree YS, Negi PS. Effect of licorice extract on cell viability, biofilm formation and exotoxin production by *Staphylococcus aureus*. *J Food Sci Tech Mys.* 2016;53(2):1092–1100. doi:10.1007/s13197-015-2131-6
44. Zuo J, Meng T, Wang Y, Tang W. A review of the antiviral activities of glycyrrhizic acid, glycyrrhetic acid and glycyrrhetic acid monoglucuronide. *Pharmaceutical.* 2023;16(5):641. doi:10.3390/ph16050641
45. Zhao X, Zhang H, Gao YX, Lin Y, Hu J. A simple injectable moldable hydrogel assembled from natural glycyrrhizic acid with inherent antibacterial activity. *ACS Appl Bio Mater.* 2020;3(1):648–653. doi:10.1021/acsomega.9b01007
46. Qian Y, Zheng Y, Jin J, et al. Immunoregulation in diabetic wound repair with a photoenhanced glycyrrhizic acid hydrogel scaffold. *Adv Mater.* 2022;34(29):e2200521. doi:10.1002/adma.202200521

47. Selyutina OY, Polyakov NE. Glycyrrhizic acid as a multifunctional drug carrier - From physicochemical properties to biomedical applications: a modern insight on the ancient drug. *Int J Pharm.* 2019;559271–559279. doi:10.1016/j.ijpharm.2019.01.047
48. Cui L, Wang X, Liu Z, et al. Metal-organic framework decorated with glycyrrhetic acid conjugated chitosan as a pH-responsive nanocarrier for targeted drug delivery. *Int J Biol Macromol.* 2023;240124370. doi:10.1016/j.ijbiomac.2023.124370
49. Wan Z, Sun Y, Ma L. Thermoresponsive structured emulsions based on the fibrillar self-assembly of natural saponin glycyrrhizic acid. *Food Funct.* 2017;8(1):75–85. doi:10.1039/c6fo01485b
50. Saha A, Adamcik J, Bolisetty S, Handschin S, Mezzenga R. Fibrillar networks of glycyrrhizic acid for hybrid nanomaterials with catalytic features. *Angew Chem Int Ed Engl.* 2015;54(18):5408–5412. doi:10.1002/anie.201411875
51. El-Sherbiny GM, Kalaba MH, Sharaf MH. Biogenic synthesis of CuO-NPs as nanotherapeutics approaches to overcome multidrug-resistant *Staphylococcus aureus* (MDRSA). *Artif Cell Nanomed B.* 2022;50(1):260–274. doi:10.1080/21691401.2022.2126492
52. Liu W, Li Z, Wang Z, et al. Functional system based on glycyrrhizic acid supramolecular hydrogel: toward polymorph control, stabilization, and controlled release. *ACS Appl Mater Interfaces.* 2023. doi:10.1021/acsami.2c19903
53. Fan Z, Cheng P, Chu L, Han J. Exploring the rheological and structural characteristics of novel pectin-salcan gels. *Polymers.* 2022;14(21):4619. doi:10.3390/polym14214619
54. Thambi T, Li Y, Lee DS. Injectable hydrogels for sustained release of therapeutic agents. *J Control Release.* 2017;26757–26766. doi:10.1016/j.jconrel.2017.08.006
55. Dong Q, Zu D, Kong L, et al. Construction of antibacterial nano-silver embedded bioactive hydrogel to repair infectious skin defects. *Biomater Res.* 2022;26(1):36. doi:10.1186/s40824-022-00281-7
56. Brown NM, Goodman AL, Horner C, Jenkins A, Brown EM. Treatment of methicillin-resistant *Staphylococcus aureus* (MRSA): updated guidelines from the UK. *JAC Antimicrob Resist.* 2021;3(1):dlaa114. doi:10.1093/jacamr/dlaa114
57. Lagies S, Pichler R, Vladimirov G, et al. Metabolic and lipidomic assessment of kidney cells exposed to nephrotoxic vancomycin dosages. *Int J Mol Sci.* 2021;22(18):10111. doi:10.3390/ijms221810111
58. Gao J, Hou H, Gao F. Current scenario of quinolone hybrids with potential antibacterial activity against ESKAPE pathogens. *Eur J Med Chem.* 2022;247115026. doi:10.1016/j.ejmech.2022.115026
59. Luo J, Wei W, Waldspuhl J, Moitessier N. Challenges and current status of computational methods for docking small molecules to nucleic acids. *Eur J Med Chem.* 2019;168414–168425. doi:10.1016/j.ejmech.2019.02.046
60. Wang YX, Malkmes MJ, Jiang C, et al. Antibacterial mechanism and transcriptome analysis of ultra-small gold nanoclusters as an alternative of harmful antibiotics against Gram-negative bacteria. *J Hazard Mater.* 2021;416:126236. doi:10.1016/j.jhazmat.2021.126236
61. Ahmad A, Majaz S, Nouroz F. Two-component systems regulate ABC transporters in antimicrobial peptide production, immunity and resistance. *Microbiology.* 2020;166(1):4–20. doi:10.1099/mic.0.000823
62. Mohammed EAH, Peng Y, Wang Z, Qiang X, Zhao Q. Synthesis, antiviral, and antibacterial activity of the glycyrrhizic acid and glycyrrhetic acid derivatives. *Russ J Bioorg Chem.* 2022;48(5):906–918. doi:10.1134/S1068162022050132
63. Pastorino G, Cornara L, Soares S, Rodrigues F, Oliveira M. Liquorice (*Glycyrrhiza glabra*): a phytochemical and pharmacological review. *Phytother Res.* 2018;32(12):2323–2339. doi:10.1002/ptr.6178
64. Li Q, He Q, Xu M, et al. Food-grade emulsions and emulsion gels prepared by soy protein-pectin complex nanoparticles and glycyrrhizic acid nanofibrils. *J Agric Food Chem.* 2020;68(4):1051–1063. doi:10.1021/acs.jafc.9b04957
65. Cai DS, Yang YQ, Lu JH, et al. Injectable carrier-free hydrogel dressing with anti-multidrug-resistant *Staphylococcus aureus* and anti-inflammatory capabilities for accelerated wound healing. *ACS Appl Mater Inter.* 2022. doi:10.1021/acsami.2c15463

International Journal of Nanomedicine

Dovepress

## Publish your work in this journal

The International Journal of Nanomedicine is an international, peer-reviewed journal focusing on the application of nanotechnology in diagnostics, therapeutics, and drug delivery systems throughout the biomedical field. This journal is indexed on PubMed Central, MedLine, CAS, SciSearch®, Current Contents®/Clinical Medicine, Journal Citation Reports/Science Edition, EMBASE, Scopus and the Elsevier Bibliographic databases. The manuscript management system is completely online and includes a very quick and fair peer-review system, which is all easy to use. Visit <http://www.dovepress.com/testimonials.php> to read real quotes from published authors.

Submit your manuscript here: <https://www.dovepress.com/international-journal-of-nanomedicine-journal>